IJCRT.ORG ISSN : 2320-2882

INTERNATIONAL JOURNAL OF CREATIVE RESEARCH THOUGHTS (IJCRT)

An International Open Access, Peer-reviewed, Refereed Journal

SOLAR BASED HIGH STEPUP TRANSFORMERLESS STANDALONE INVERTER USING CONTROL TECHNIQUES

[1] TAMILARASAN K, [2] Dr. GEETHA V

[1] PG scholar, [2] Professor and Head,

[1] Department of Electrical and Electronics Engineering,

[1] Government College of Engineering, Salem, Tamil Nadu, India

Abstract: This paper presents the simulation and implementation of a solar based high stepup transformerless standalone inverter using control techniques. The proposed topology is a two-stage (DC-DC-AC) power conversion topology. In this proposed topology a non-isolated high stepup DC-DC Quadratic Boost converter is coupled with a dynamic dc-link single phase inverter. The front-end Quadratic boost converter is controlled by fuzzy logic controller based Perturb and Observe (P&O) MPPT control technique and the inverter stage is controlled by PR controller based current and voltage control techniques. The performance of the proposed Quadratic boost converter fed inverter configurations is validated through simulation in MATLAB/Simulink platform for hardware implementation, the proposed control techniques are programmed in dsPIC30f2010 Digital Signal Controller. The proposed FLC -P&O MPPT control technique have high efficiency, low overshoot and less oscillation time compared to conventional P&O MPPT technique. The proposed Quadratic boost converter proves good steady state performance, low voltage ripple, current ripple and preserve constant output voltage with the help of FLC. The proposed PR controller based current and voltage control techniques are used to control the inverter output voltage and current by changing the modulation index and maintain zero steady state error in sinusoidal quantities compared to PI controller. The proposed inverter proves good steady state performance, low THD, and preserve constant output voltage with the help of PR controller. The FLC controller and PR controller-based control techniques are increases the efficiency and reduce the THD range within 5% of the proposed model.

Index Terms **- FLC based P&O MPPT, PR Controller, Quadratic Boost converter, Transformerless stand-alone Inverter, Unipolar SPWM, Low Harmonic distortion, MATLAB/Simulink.**

I. INTRODUCTION

In recent years, many research works have been done on the use of solar photovoltaic (PV) energy as an alternative energy resource. PV energy is one of most hopeful renewable energy resources and it is clean and pollution free [1]-[2]-[3]. There are two different type of power conversion topologies such as isolated and non-isolated configuration [1]-[5]. Due to use of transformer in the isolated inverter structure, there are some drawbacks such as low power density and complicated to control the output [1]-[4]-[5]. The conventional P&O MPPT have low MPPT ratio, more oscillation time and high overshoot voltage [2]-[7]. Due to these drawbacks the output power efficiency will be very low and it affects the efficiency of the system [1]-[8]-[11].

The Fuzzy logic controller-based P&O MPPT technique have less settling time, low oscillation time and low overshoot, and is stable at change in irradiance [2]-[3]-[10]. Due to these advantages, it improves the MPPT ratio, reduce oscillation and overshoot voltage [2]-[3]-[10]-[12]. The PI controller cannot produce zero steady state error in sinusoidal quantities [4]-[18]. Due this drawback, it make overshoot voltage and also it reduces the quality of the sine wave [5]-[14]. The PR controller can maintain zero steady state error in sinusoidal quantities [4]-[5]-[19]-[20]. This paper presents work on improving MPPT algorithm which should be able to increase performance of the PV system. This paper introduces combination of features in both conventional P&O MPPT and FLC to form single algorithm for MPPT of PV dc-dc Quadratic boost converter which is simple and faster. This proposed MPPT method proves better steady state performance with various irradiance conditions. This paper introduces PR controller based Current and Voltage control techniques for stand-alone inverter to control the inverter output voltage. This proposed PR controller-based control technique proves better steady state performance. This control technique achieves zero steady state error in sinusoidal quantities. This control technique achieves zero steady state error in sinusoidal quantities. The Figure:1 shows block diagram of Proposed model. To further explain about this work, Section 2 in this paper covers configuration of Proposed model, and Quadratic boost converter discussed in Section 3, and followed by discussion on fuzzy logic controller implementation in Section 4, PR controller implementation discussed in Section 5, simulation and results are discussed in Section 6, Hardware and Results are discussed in Section 7, Finally, Section 8 concludes findings from this work.

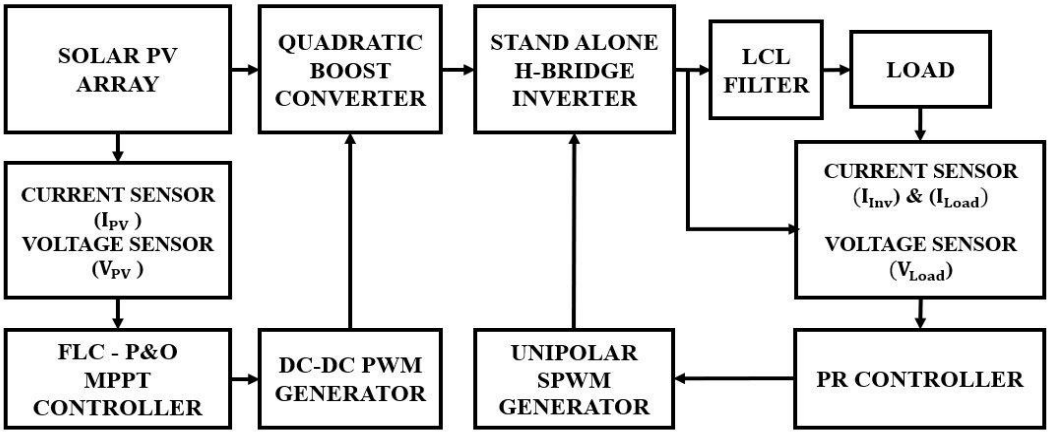

Figure:1 Block diagram of Proposed model

II. CONFIGURATION OF PROPOSED MODEL

The configuration of proposed model consists of Solar PV array, High stepup DC-DC Quadratic Boost converter and Stand-alone inverter. The proposed inverter topology is a two-stage power conversion topology is shown in figure 2. Configuration of the proposed high stepup DC-DC Quadratic boost converter fed Transformerless Inverter

A. SOLAR PV ARRAY

In this proposed model, 1SOLTECH 1STH-215-P PV panel is used with the following characteristics: Maximal Module Power ($\mathbf{P_{max}}$) of 213.15W, optimal voltage ($\mathbf{V_{mp}}$) of 29V, optimal current ($\mathbf{I_{mp}}$) of 7.35A, saturation current ($\mathbf{I_o}$) of 2.9259e−10A, photo-current ($\mathbf{I_{ph}}$) of 5.9602A, short circuit current ($\mathbf{I_{sc}}$) of 7.84A, open circuit voltage ($\mathbf{V_{oc}}$) of 36.3V, series resistance ($\mathbf{R_s}$) of 0.037998Ω, shunt resistance ($\mathbf{R_{sh}}$) of 313.3991Ω and number of cells equal to 60. As regards the PV array, it consist of series modules number of 7 and parallel modules number of 5. Hence, the PV has a power of 7× 5 × 213.15W= 7500W. Irradiance of 1kW/$\mathbf{m^2}$ and cell temperature of 25℃ are the electrical specifications under test conditions.

B. HIGH STEPUP DC-DC QUADRATIC BOOST CONVERTER

In this proposed model, dc–dc converter make use of MPPT. dc–dc converter can be used as switching-mode regulator to convert a dc voltage, normally unregulated, to a regulated dc output voltage. The regulation is normally achieved by pulse-width modulation (PWM) technique and the switching device is normally ON. Quadratic Boost dc–dc converter's function is to step up dc voltage.

Maximum power is reached when the MPPT algorithm changes and adjusts the PWM's duty cycle of the Quadratic boost dc–dc converter. The proposed FLC-P&O MPPT technique controls the Quadratic boost converter. Boost Inductor and DC link capacitor functions of Quadratic boost converter is instead defined as:

$$\text{Boost Inductor } (L_b) = \frac{(V_{out} - V_{in})\ V_{in}}{f_{sw} \times \Delta I \times V_{out}} \quad (1)$$

$$\text{DC link capacitor } (C_{dc}) = \frac{(V_{out} - V_{in})\ I_{out}}{f_s \times \Delta V \times V_{out}} \quad (2)$$

where $\mathbf{f_s}$-Switching frequency ($\mathbf{f_s}$ =25 kHz), V_{in} and V_{out} are the input and output voltages, respectively, $\Delta\mathbf{I}$ and $\Delta\mathbf{V}$ are the inductor current and voltage ripple. The value of Boost inductor is 10.89mH and dc-link capacitor is about 1000μF.

C. STAND ALONE INVERTER

In this proposed model, closed loop (stand-alone) single phase inverter stage is directly coupled with dc–dc converter. The proposed inverter output voltage and current are controlled by PR controller-based control technique. In this inverter voltage and current control is normally achieved by Unipolar sinusoidal pulse-width modulation (SPWM) technique. This inverter can convert 400V DC voltage into 230V (RMS) AC voltage using PR controller

To design a LC filter by using this formula,

$$\text{Cut off frequency } (\mathbf{f_c}) \leq \frac{f_{sw}}{10} \quad (3)$$

$$\text{Filter Inductor } (L_f) < \frac{0.03\ V_{out}}{(2\pi f_c)\ I_{Lmax}} \quad (4)$$

$$\text{Filter Capacitor } (C_f) = \frac{1}{(2\pi f_c)^2\ Lf} \quad (5)$$

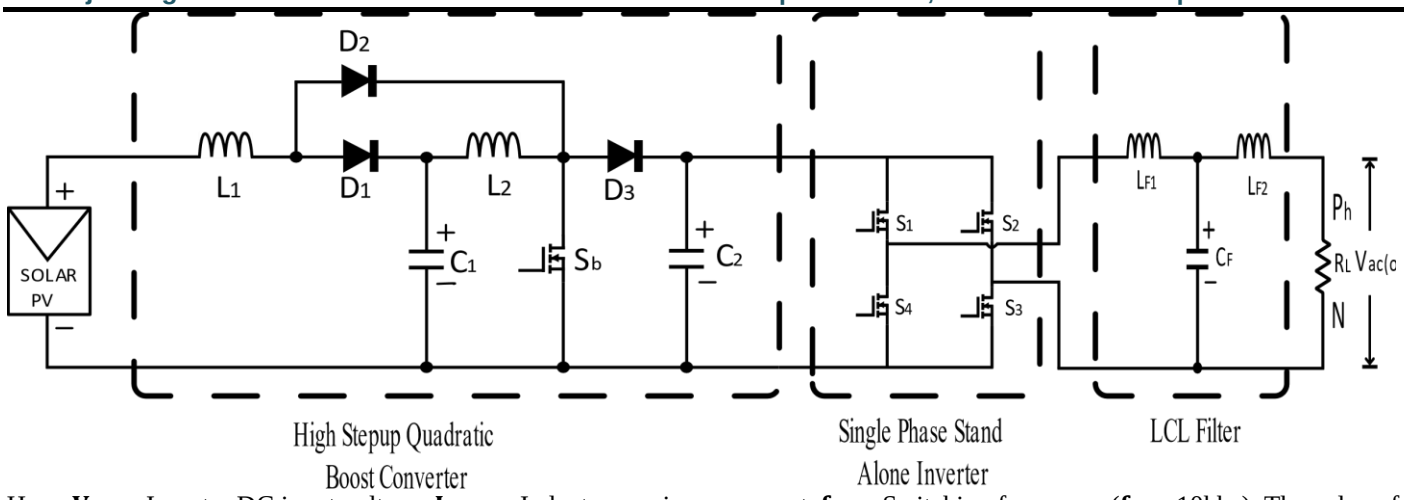

Here, $\mathbf{V_{out}}$ – Inverter DC input voltage, $\mathbf{I_{Lmax}}$ – Inductor maximum current, $\mathbf{f_{sw}}$ – Switching frequency ($\mathbf{f_{sw}}$= 10khz). The value of filter inductor is 4.06mH and the filter capacitor is about 6.23 μF.

Figure:2 Configuration of the proposed high stepup DC-DC Quadratic boost converter fed Transformerless inverter

III. QUADRATIC BOOST CONVERTER

In PWM (square-wave) dc-to-dc converter topologies, dc conversion ratio M is a function of duty ratio D of the active (transistor) switch. Both minimum and maximum attainable conversion ratios are limited in practical converters. M_{max} is limited by the degradation in efficiency as duty ratio D approaches 1. On the lower end, minimum ON-time of the transistor switch results in a minimum attainable duty ratio and, consequently, in a minimum conversion ratio $M_{min.}$ Conversion range can be extended significantly if conversion ratio M has a quadratic dependence on duty-cycle. Quadratic boost converter (QBC) is a modified step up converter with single switch and better conversion ratio.

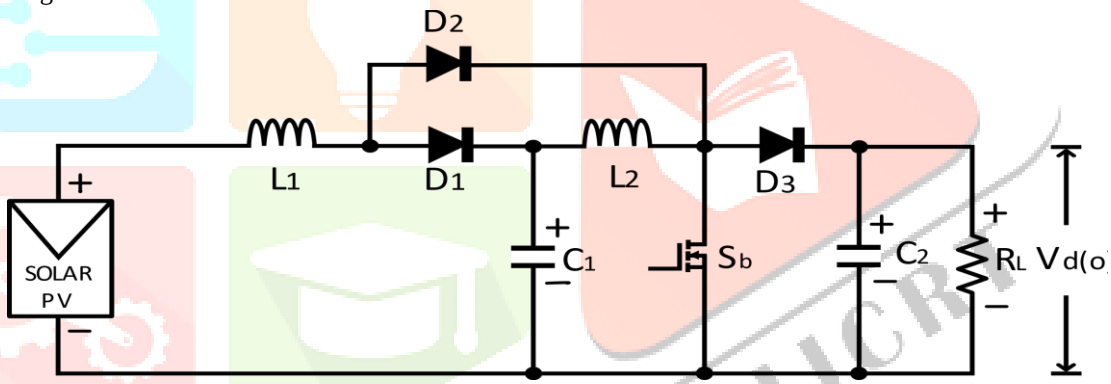

Figure 3: Quadratic boost converter

The circuit diagram of a quadratic boost converter [3] is shown in Figure 3. The circuit diagram of a quadratic boost converter. The circuit comprises of a single power MOSFET switch, S, two diodes, D_1 and D_2, two capacitors, C_1 and C_2, two inductors L_1 and L_2 and a load resistor R.

The circuit operation is strictly based on the assumption that the switch S is ideal in operation and capacitors C_1 and C_2 is assumed to be large so that the voltage across the capacitors V_{C1} and V_{C2} are nearly constant over a switching period. When the switch is ON: The equivalent circuit schematic of the QBC during the ON state is shown in Figure 4. when switch S is turned on D_2 is forward biased, whereas D_1 and D_3 reverse biased. Currents are supplied to L_1 and L_2 by Vin and C_1 respectively.

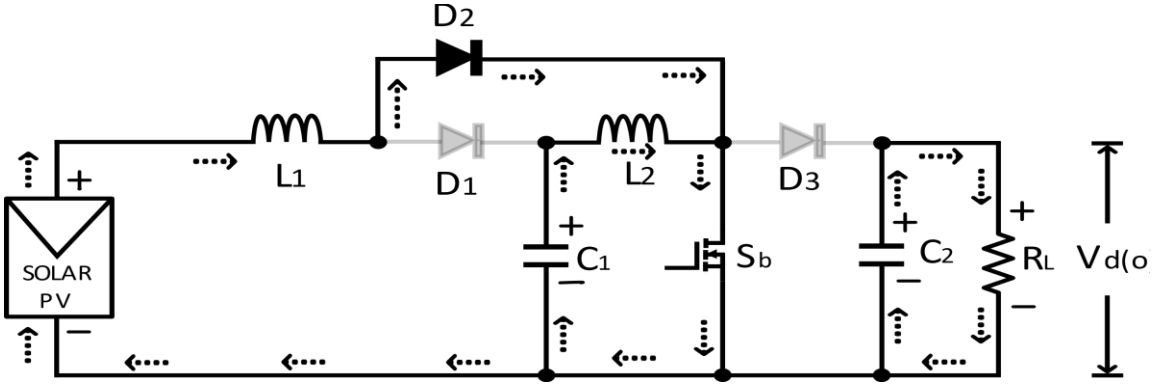

Figure 4: Quadratic boost converter when switch is ON

When the switch is OFF: The way of operation and current flow direction of QBC during OFF state is shown in Figure 5. In this condition D1 and D3 are forward biased, whereas D2 reverse biased. L1 and L2 are charging C1 and C2 respectively. During this state, iL1 and iL2 is decreased

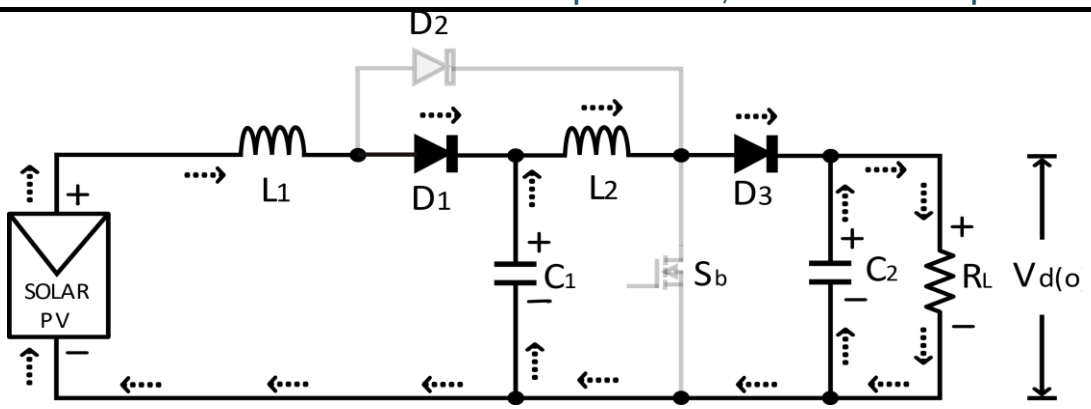

Figure 5: Quadratic boost converter when switch is OFF

A. STEADY STATE ANALYSIS OF QUADRATIC BOOST CONVERTER

The relationship between inputs (V_{in}) and outputs (V_{out}) variables of the Quadratic boost converter is represented by the following equations

The basic circuit of Quadratic boost converter constitutes a boost converter with an assumption of purely resistive load, ideal switch and a constant instantaneous input voltage V_d. Since in steady state operation the waveforms must repeat from one time period to next, the integral of the inductor voltage V_{L1} and V_{L2} over one time period must be zero.

$\int_0^{Ts} \boldsymbol{V}L1 = 0$ …….. (6)

$\int_0^{Ts} \boldsymbol{V}L2 = 0$ …….. (7)

The expansion of the above two equation gives voltage gain equation as shown in Equation (8)

$\frac{\boldsymbol{Vo}}{\boldsymbol{Vd}} = \frac{\mathbf{1}}{(\mathbf{1-D})^2}$ …….. (8)

At steady state the net charge in the capacitor current is zero. In other words integral of each capacitor current over one switching period Ts must be zero.

$\int_0^{Ts} \boldsymbol{i}c1 = 0$ …….. (9)

$\int_0^{Ts} \boldsymbol{i}c2 = 0$ …….. (10)

By expanding the above equation, the value of inductor current I_{L1} and I_{L2} is obtained as follows,

I L1= $\frac{\boldsymbol{I_0}}{(\mathbf{1-D})^2}$ …….. (11)

I L2= $\frac{\boldsymbol{I_0}}{(\mathbf{1-D})^2}$ …….. (12)

B. QUADRATIC BOOST INDUCTOR AND DC LINK CAPACITOR DESIGN

Boost Inductor (L_b) and DC link capacitor (C_{dc}) functions of the DC-DC Quadratic boost converter are instead defined as:

$L_1, L_2 = \frac{\mathbf{Vs(min)*D}}{\boldsymbol{Fs*\Delta IL}}$ Henry …….... (13)

$= \frac{\mathbf{203*0.3}}{\mathbf{30*10^3*0.02}}$ Henry

= 101.5mH

L_1, L_2 = 101.5mH

$C_1, C_2 = \frac{\mathbf{Io(max)*D}}{\boldsymbol{Fs*\Delta Vc}}$ Farad ……. (14)

$= \frac{\mathbf{18.75*0.54325}}{\mathbf{30*10^3*0.05}}$

C_1, C_2 = 3.75 Microfarad

Here:

D - Duty cycle

$\boldsymbol{F_{sw}}$- Switching frequency (In simulation and hardware $\boldsymbol{F_{sw}}$ = 30kHz)

V_{in} - Input voltage (Vin = 100 to 200V)

V_{out} - Output voltages (Vout = 400V)

I_{in} – Input current (Iin = 30A)

I_{out} – Output current (Iout = 15A)

ΔI - Current ripple (2% of output current)

ΔV - Voltage ripple (5% of output voltage)

The value of boost inductor is L_1 , L_2 = 101.5mH

and DC link capacitor is C_2 = 375µF.

Output filter Capacitor, C_1, C_2 = 3. 75mf

IV. FUZZY LOGIC CONTROLLER IMPLEMENTATION

A fuzzy inference system (FIS) is mathematical means of describing vagueness in linguistic terms. instead of exact mathematical description. They are appropriate dealing with uncertainties and approximate reasoning. Membership function ranges from 0-1 in their linguistic from associated with imprecision concept. A FLC-P&O MPPT is more stable and it have low oscillation

time compared to conventional P&O MPPT controller. A FLC is divided into four categories, which include fuzzification, fuzzy inference, rule-base and defuzzification.

A. FLC-P&O MAXIMUM POWER POINT TRACKING

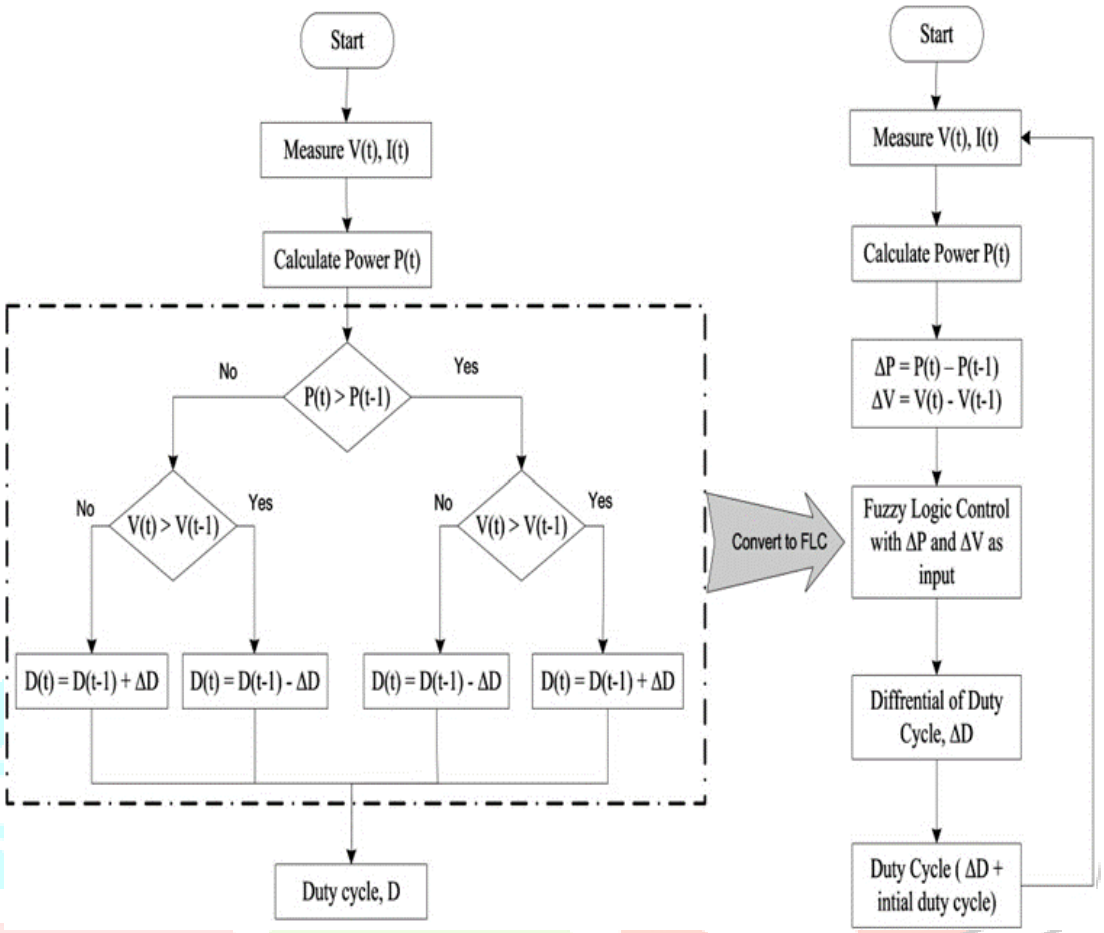

Figure:6 Comparison between P&O and FLC- P&O MPPT

The conventional and popular Maximum Power Point Tracking technique is P&O MPPT algorithm. The voltage is perturbed and the change of the output power is observed so it is called P&O MPPT algorithm. The inputs of the P&O algorithm are PV current and voltage. The proposed FLC-MPPT technique uses inputs of P&O algorithm such as differential power ΔP and differential voltage ΔV. The proposed change in this algorithm is to replace comparing and switching methods with fuzzy logic approach, as shown in Figure:6 shows Comparison between P&O and FLC- P&O MPPT and Figure:7 shows implementation of the algorithm in MATLAB-Simulink.

During fuzzification, the numerical input variables are converted into linguistic variables based on the membership functions. Various fuzzy levels could be used for input and output variables. Five proposed fuzzy sets for input and output variables are N (negative), ZE (zero), PS (positive small), P (positive) and PB (positive big). Figure :8 shows membership functions for input of difference between the current power and the previous power ΔP, input of difference between the current voltage and the previous voltage ΔV and output of difference between the current duty cycle and the previous duty cycle ΔD. After ΔP and ΔV are calculated, they are converted into linguistic variables and then the output ΔD is generated by looking up in a rule-base table as shown in Table 1, which consists of 25 rules. This algorithm uses Mamdani fuzzy inference system to determine the output. Usually, weights are added to the rules to improve reasoning accuracy and to reduce undesirable consequent. The fuzzy output is converted back to numerical variable from linguistic variable during defuzzification. In this algorithm uses method the common COA is used for the defuzzification.

In its operation, when ΔP and ΔV are either positive or negative values, the FLC will decide the best and accurate value of ΔD. Therefore, ΔD will be changed according to the condition of ΔP and ΔV at certain time where measurement process is done. It will obey the membership function designed in the proposed FLC.

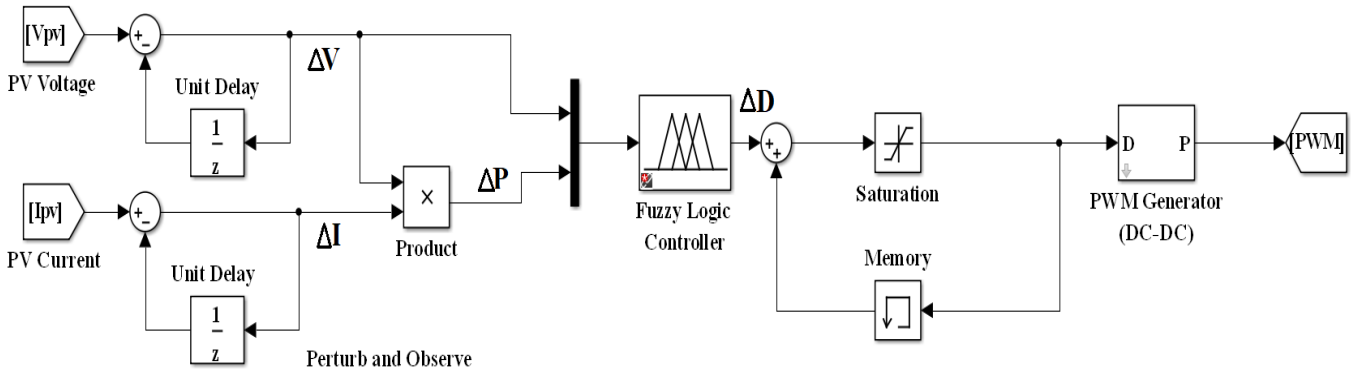

Figure:7 Implementation of the FLC_P&O MPPT algorithm in MATLAB-Simulink

Table 1 Fuzzy Rules

ΔP\ΔV	**N**	**ZE**	**PS**	**PS**	**PB**
N	NE	PS	P	PB	PB
NE	NE	ZE	PS	P	PB
PS	N	ZE	ZE	PS	P
P	N	N	ZE	ZE	PS
PB	N	N	N	ZE	ZE

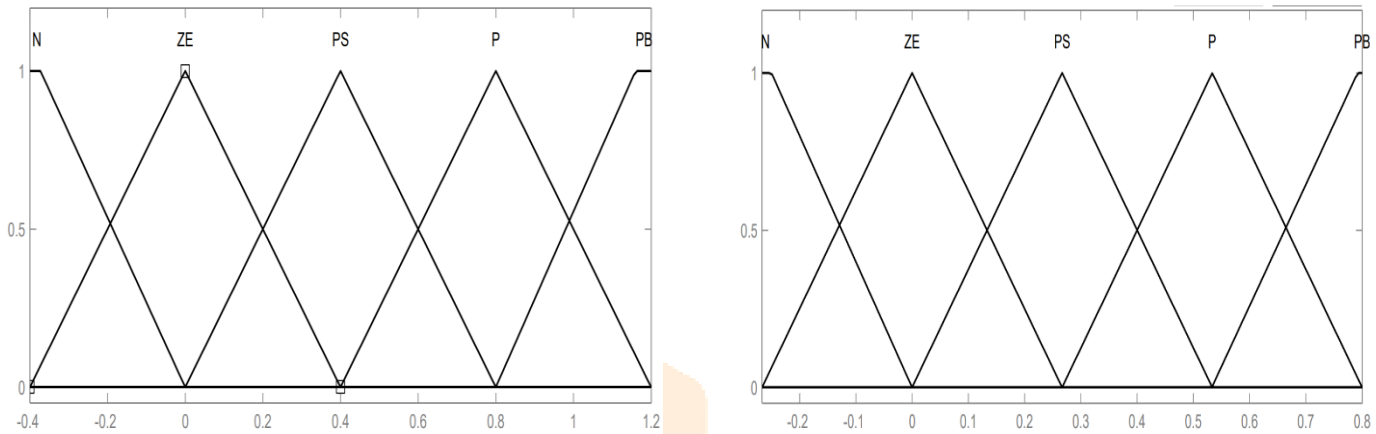

Figure:8 Membership function. a. Input of ΔP and ΔV, b. output of ΔD

V. PR CONTROLLER IMPLEMENTATION

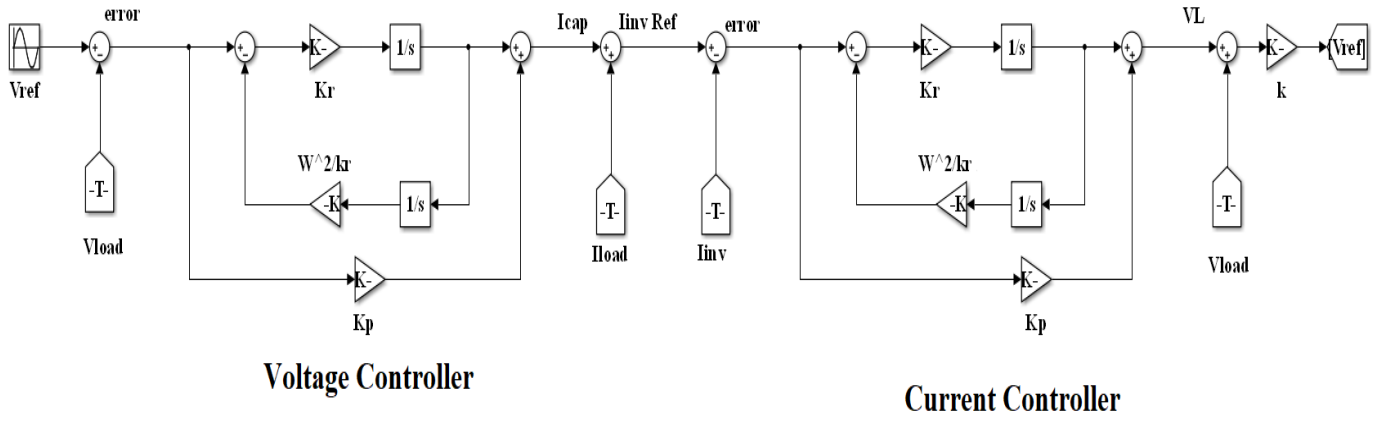

Figure:9 PR Controller block diagram

The Proportional Resonant (PR) Controller is used as output voltage controller and current controller. By comparison with the conventional PI control method, the PR control can introduce an infinite gain at the fundamental frequency and hence can achieve zero steady state error in sinusoidal quantities and this controller has additional negative feedback loop. This feedback loop makes controller performance better when compared to PI controller. For implementation of closed loop control following three voltage and current values are needed 1. output voltage or load voltage (V_{load}), 2. inverter (I_{inv}), 3. load current (I_{load}).

In voltage controller side, find the error between the sine wave reference voltage and actual load voltage (V_{load}) now the error is fed to the PR controller. Output of the controller give capacitor current (I_{cap}) now the capacitor current is added to load current according to the Kirchhoff's current law (KCL) sum of the capacitor current and load current will give reference inverter current ($I_{inv\ Ref}$).

In In current controller side, the inverter reference current ($I_{inv\ Ref}$) is compared to actual inverter current (I_{inv}) it gives error signal; the error signal is fed to PR controller. Output of the PR controller is given voltage across inductor (V_L) now add the voltage across inductor (V_L) to load voltage (V_{load}). According to Kirchhoff's Voltage law (KVL) this will give reference inverter voltage (Vref) and this is the voltage to be generated by the inverter and this voltage act as the reference voltage for Unipolar SPWM generation block, as shown in Figure:9 PR controller block diagram.

Transfer function

$$Y(s) = E(s) * \left(k_P + \frac{k_r s}{s^2+\omega^2}\right) \text{..... (15)}$$

Calculation of Proportional gain (kp) value for Voltage Controller

Controller Time Constants = 200µs

Filter Capacitance (C_f)= 6.23µF

$$k_p = \frac{\text{Capacitance}}{\text{Time Constant}} = \frac{6.23\times10^{-6}}{200\times10^{-6}} = 0.03115$$

Calculation of Proportional gain (kp) value for Current Controller

Controller Time Constants = 150µs

Filter Inductor (L_f) = 4.06mH

Inductor series resistance = 0.001

$$k_p = \frac{\text{Inductance}}{\text{Time Constant}} = \frac{4.06\times10^{-3}}{150\times10^{-6}} = 27.066$$

Calculation of Resonant gain (kr) value for Current Controller

Gain of the PR controller (G_n) $= \frac{k_r\omega_n}{\omega_n^2-\omega^2}$ **..... (16)**

Resonant frequency (ω_n) $= \frac{1}{\sqrt{LC}}$ **..... (17)**

Natural frequency (ω) = $2\times\pi\times50$**..... (18)**

kr value for current controller = 100

$$\frac{\omega^2}{k_r} = \frac{(2\times\pi\times50)^2}{100} = 986.83$$

kr value for voltage controller = 400

$$\frac{\omega^2}{k_r} = \frac{(2\times\pi\times50)^2}{400} = 246.7$$

If Vout = 400v set k = 1/400

VI. SIMULATION RESULTS AND ANALYSIS

The proposed model has been developed and simulated in Matlab/Simulink Platform. The Simulation diagram of proposed high stepup DC-DC Quadratic boost converter fed transformerless inverter is shown in Figure:10. The circuit components are obtained from Sim Power System library. A fuzzy logic controller is designed by fuzzy logic controller designer application in Matlab/Simulink Platform, refer section 2 for design a FLC. A PR controller is developed by Matlab/Simulink Platform refer section 3 for PR controller implementation. In PR controller, sine wave reference amplitude value is 230 for 230V (RMS) output, frequency value is 314.4(rad/sec). In unipolar SPWM, the repeating sequence time value is (0, 0.00005, 0.0001) and output value is (-1,1, -1). Scope is used for viewing the simulation results. The proposed Quadratic boost converter is simulated at a switching frequency of 25kHz. The proposed inverter is simulated at a switching frequency of 10kHz. The values of circuit components for the simulation are selected based on the design considerations and are listed in Table:2 shown below. Table:3 lists the specifications of the proposed model. The discrete state variable model of sampling time TS= 1e-06 sec is used for simulation. The various waveforms for the proposed converter and inverter are shown in Figure:11 – Figure:17 respectively. The output DC and AC voltage are compared with that of the conventional MPPT, Voltage and control schemes.

The simulation results demonstrate that the proposed model shows improved voltage gain compared to that of conventional boost converter, improved MPPT ratio and zero steady state error compared to P&O MPPT and PR controller preserve zero steady state error in sinusoidal quantities compared to PI based control technique.

Table:2 Simulation Parameters of proposed model

Circuit components	Values
Input Capacitor (C_{in})	1000µF
Inductor (L_b)	10.45mH
DC link Capacitor (C_{dc})	1000µF
Filter Inductor (L_f)	4.06mH
Filter Capacitor (C_f)	6.23µF
Load Resistor (R_{load})	56Ω

Table:3 Specifications proposed model

Specifications	Values
Solar Input voltage (Vin)	(150-260) V (DC)
Quadratic Boost converter Output voltage (Vout)	(220-400) V (DC)
Inverter output voltage (Vinv), (Vload)	(220-400) V (AC)
Maximum Power (Pm)	7500W

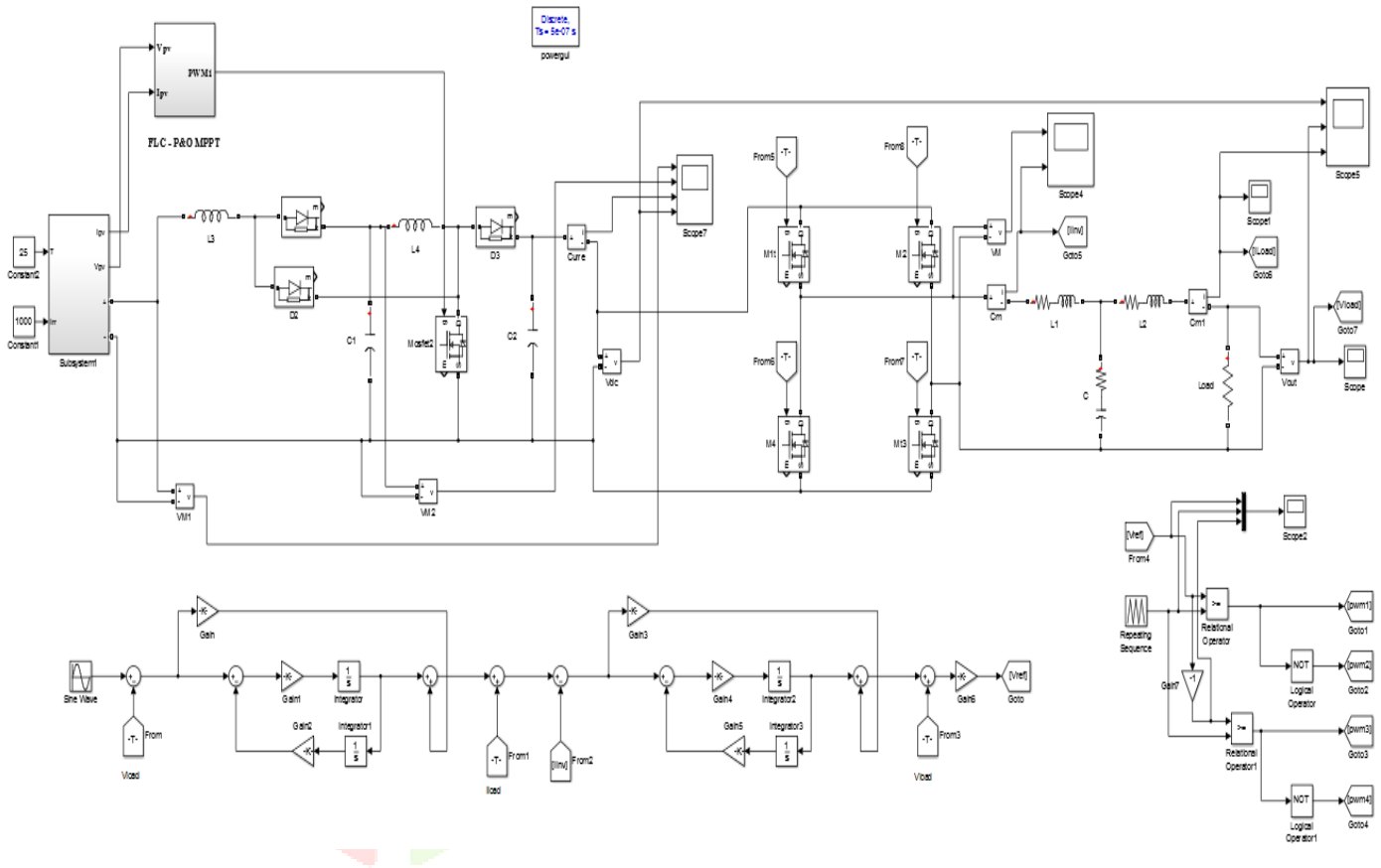

Figure:10 Simulation diagram of proposed high stepup DC-DC Quadratic boost converter fed Transformerless inverter

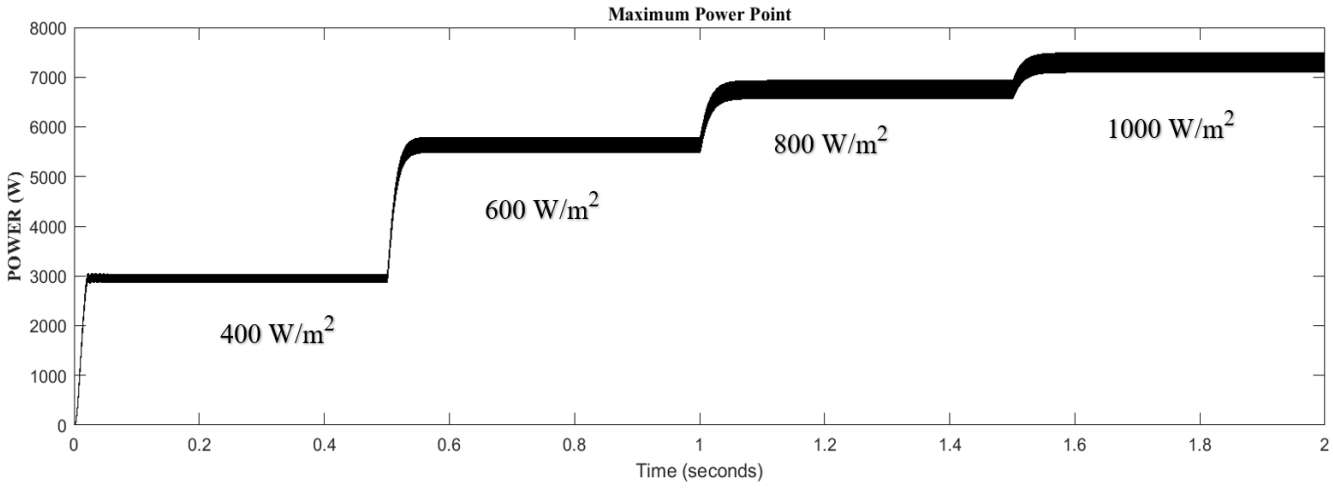

Figure:11 Maximum power point waveform of proposed FLC-P&O MPPT at change in Irradiance with Pmax = 7500W

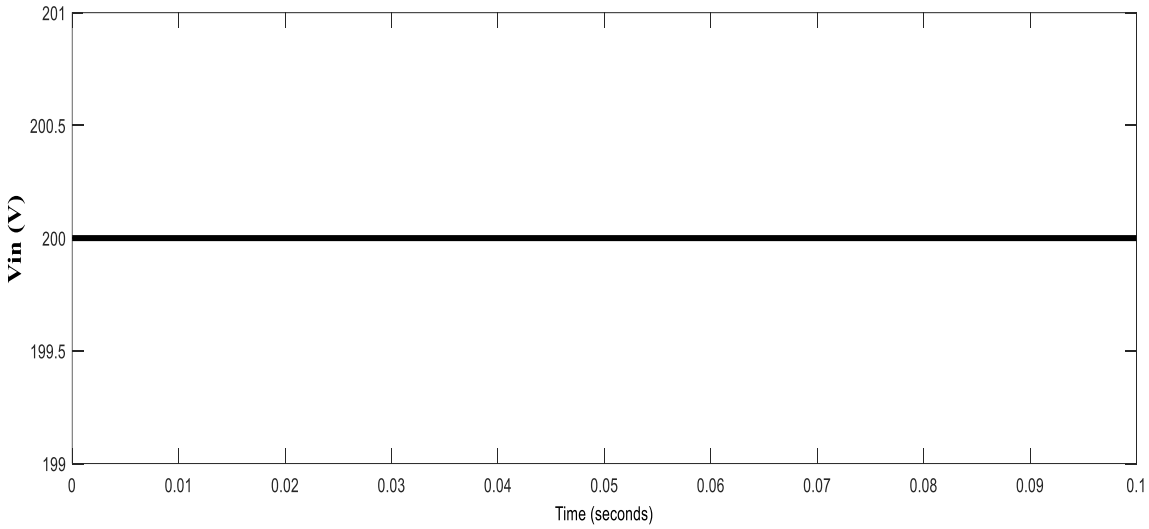

Figure:12 Input DC voltage waveform of proposed Quadratic Boost converter Vin=200V, at Irradiance of 1kW/m^2 and cell temperature of 25℃

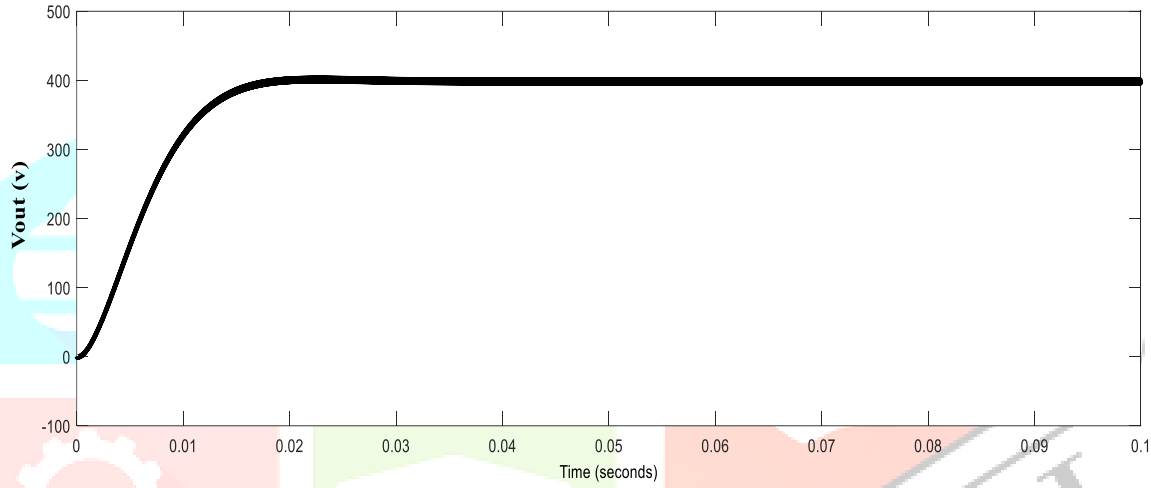

Figure:13 Output Voltage waveform of proposed Quadratic Boost converter with duty cycle D=0.5, V_{out}=400V

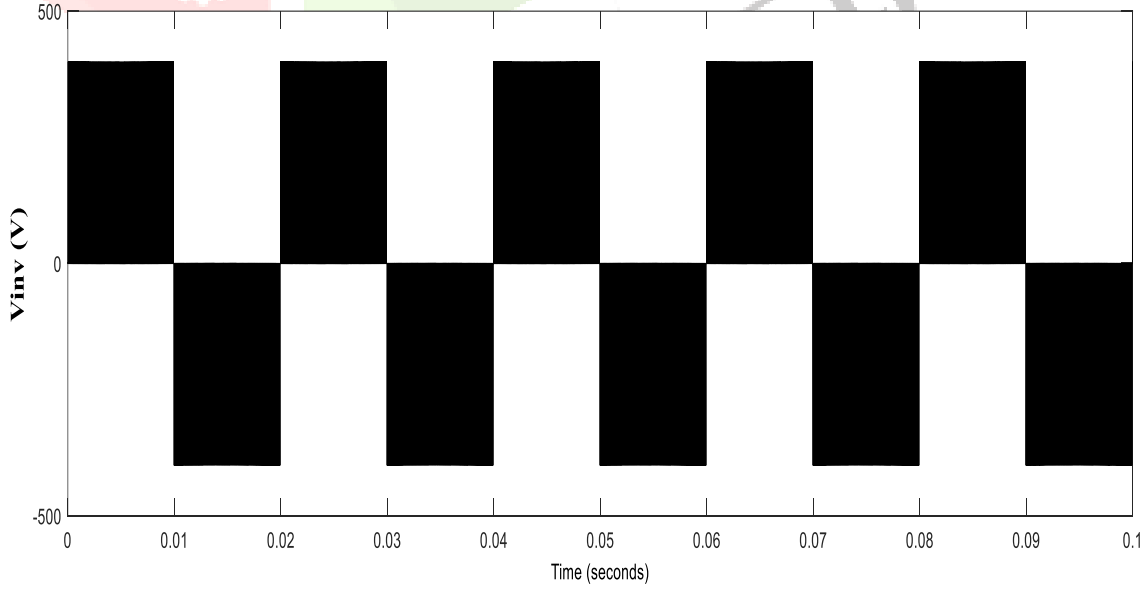

Figure:14 Before filter output voltage waveform of proposed inverter with V_{inv}=400V

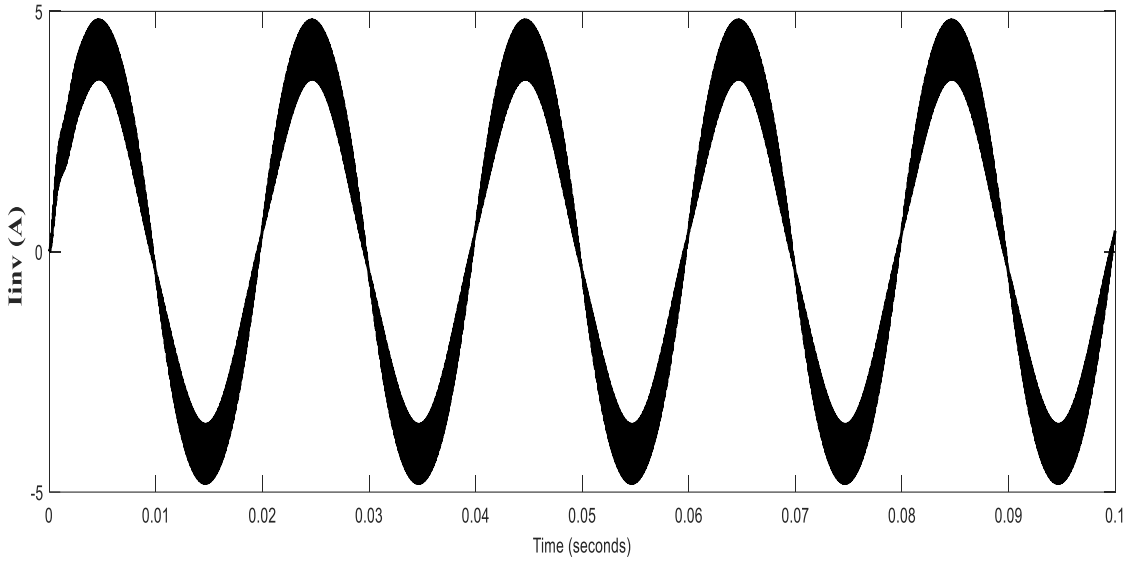

Figure:15 Before filter output current waveform of proposed inverter with I_{inv}=4.3A

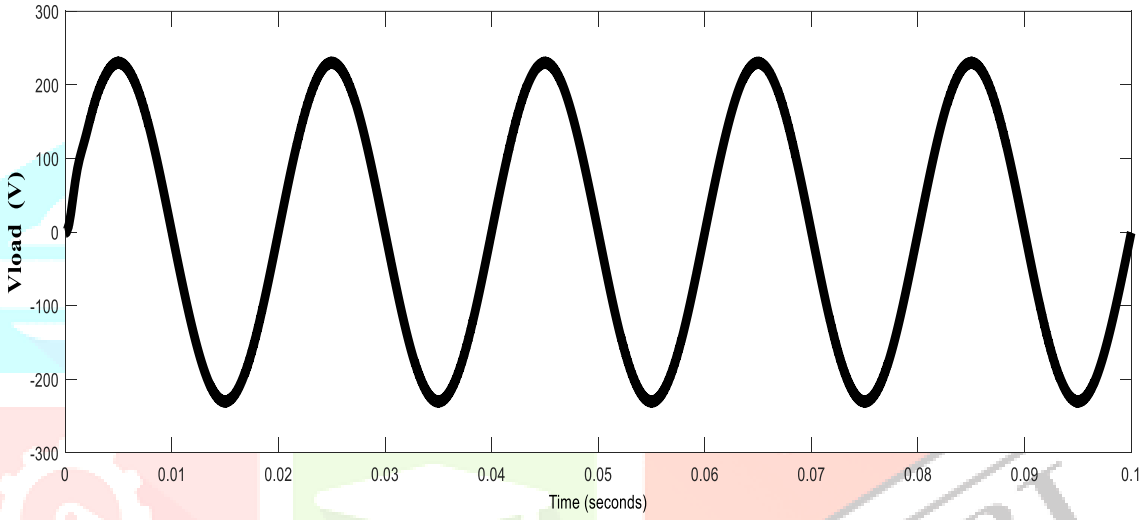

Figure:16 After filter output voltage waveform of proposed inverter with V_{load}=230V (RMS)

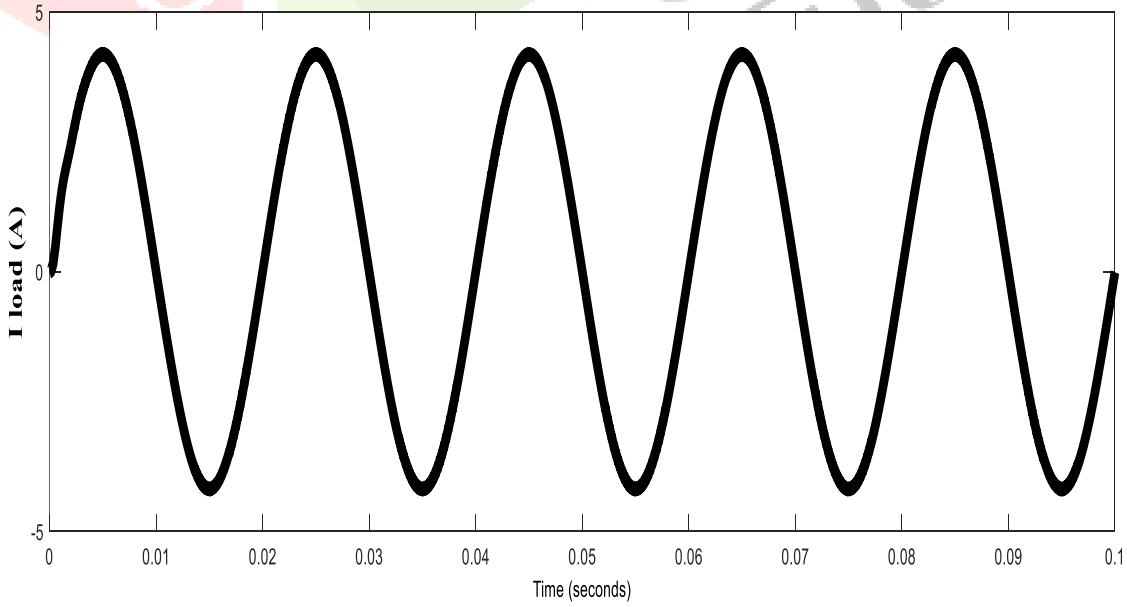

Figure:17 After filter output current waveform of proposed inverter with Iload=4.258 A (RMS)

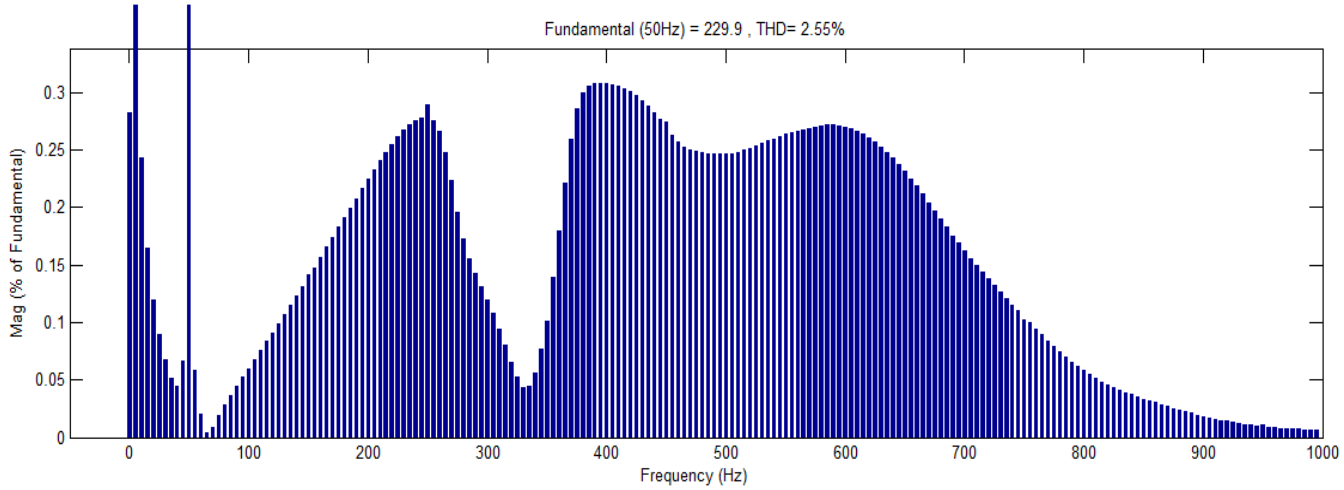

Figure:18 FFT analysis and THD value of proposed inverter output voltage with THD=2.55%

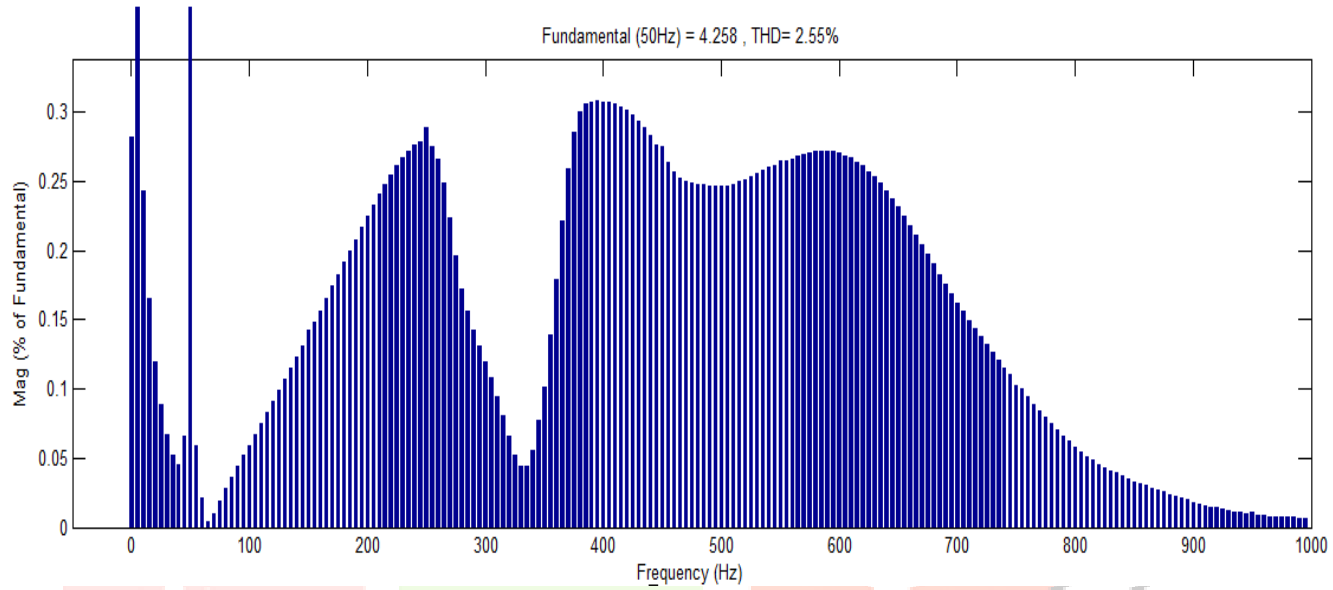

Figure:19 FFT analysis and THD value of proposed inverter output current with THD=2.55%

VII. HARDWARE RESULT

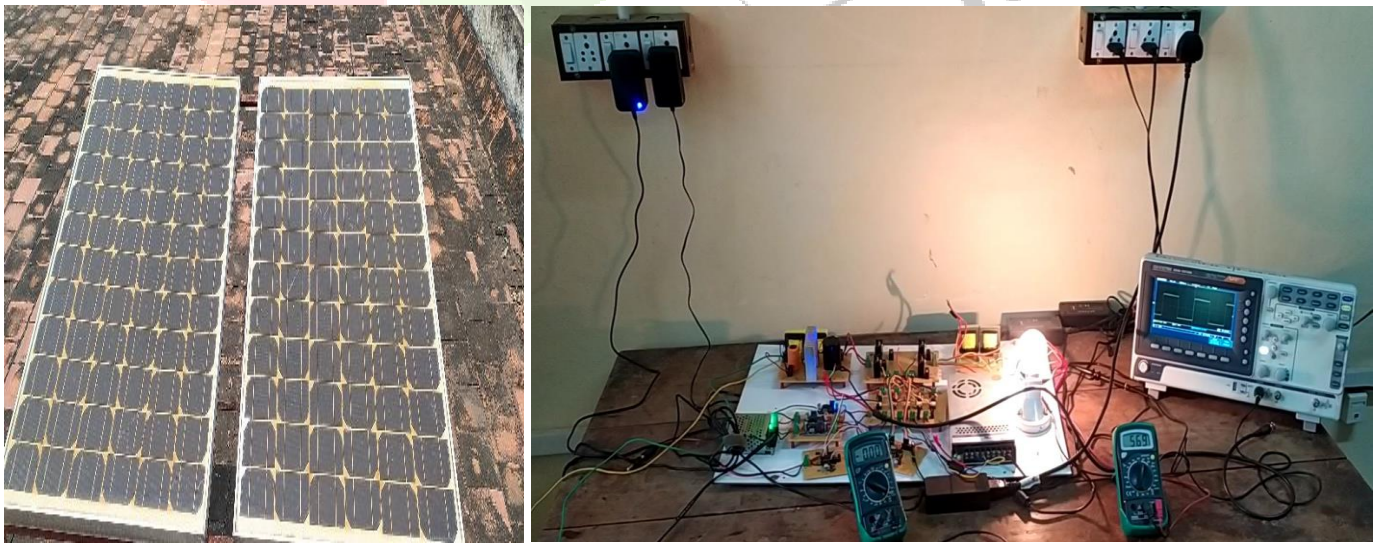

Figure :20 Hardware prototype model of solar based high stepup transformerless standalone inverter using control techniques

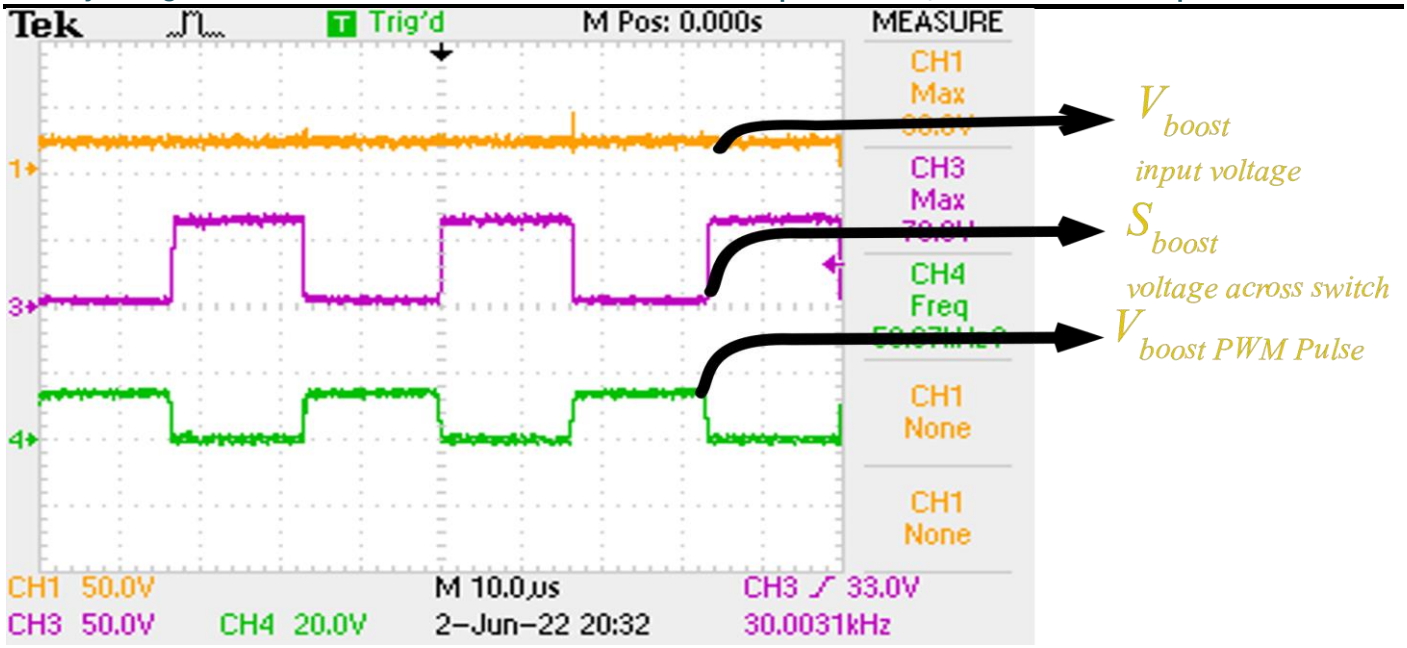

Figure :21 Proposed Quadratic boost converter input voltage and voltage stress across switch S_b, Gate pulse S_b

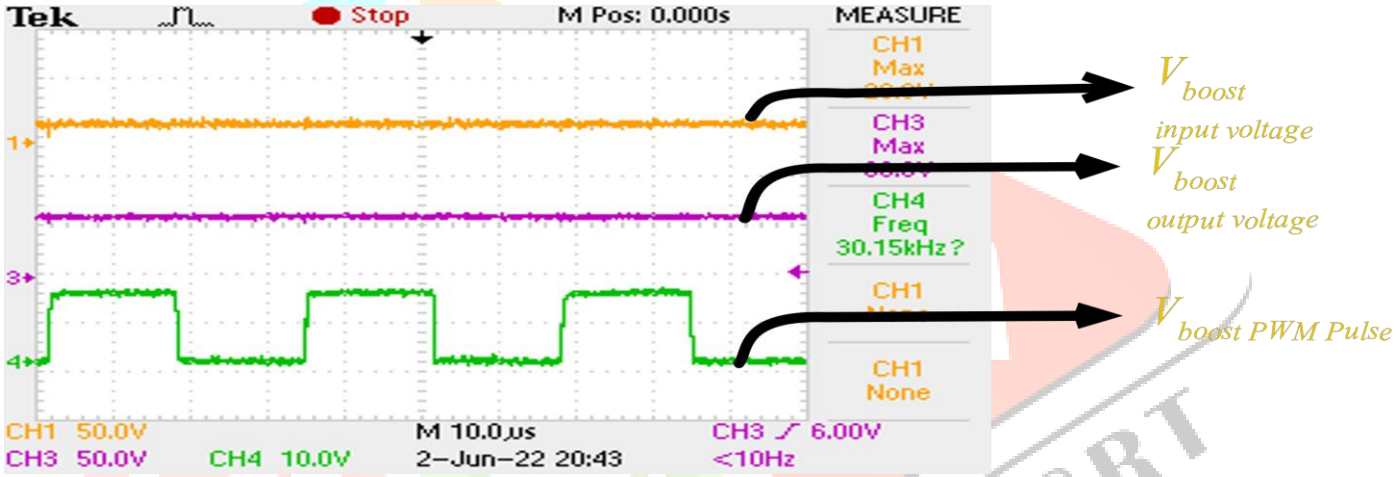

Figure :22 Proposed Quadratic boost converter input and output voltage and Gate pulse S_b

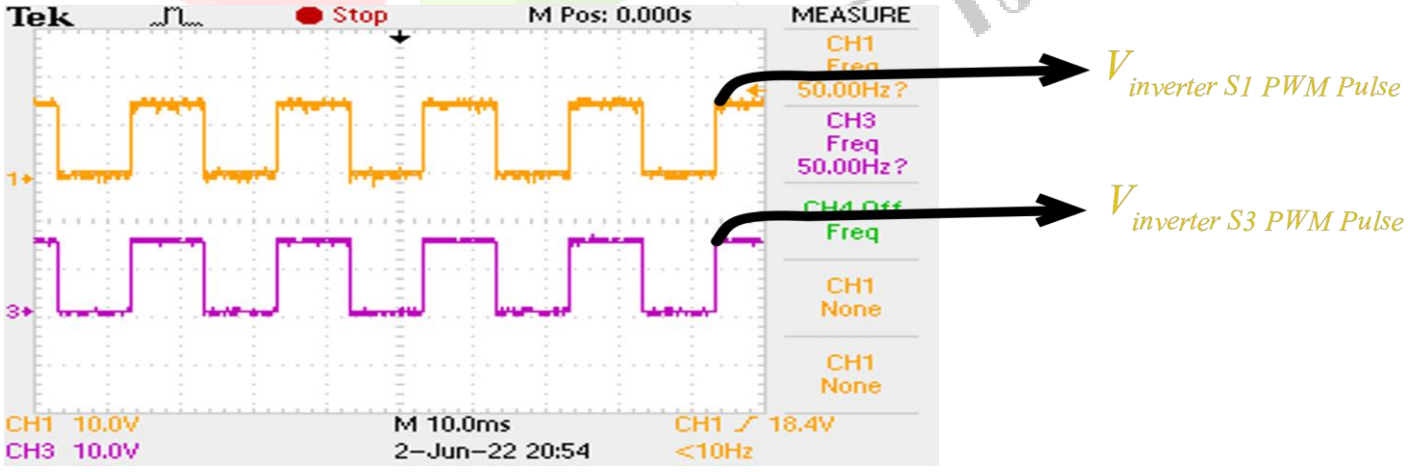

Figure :23 Proposed inverter Gate Pulse for S_1 and S_3

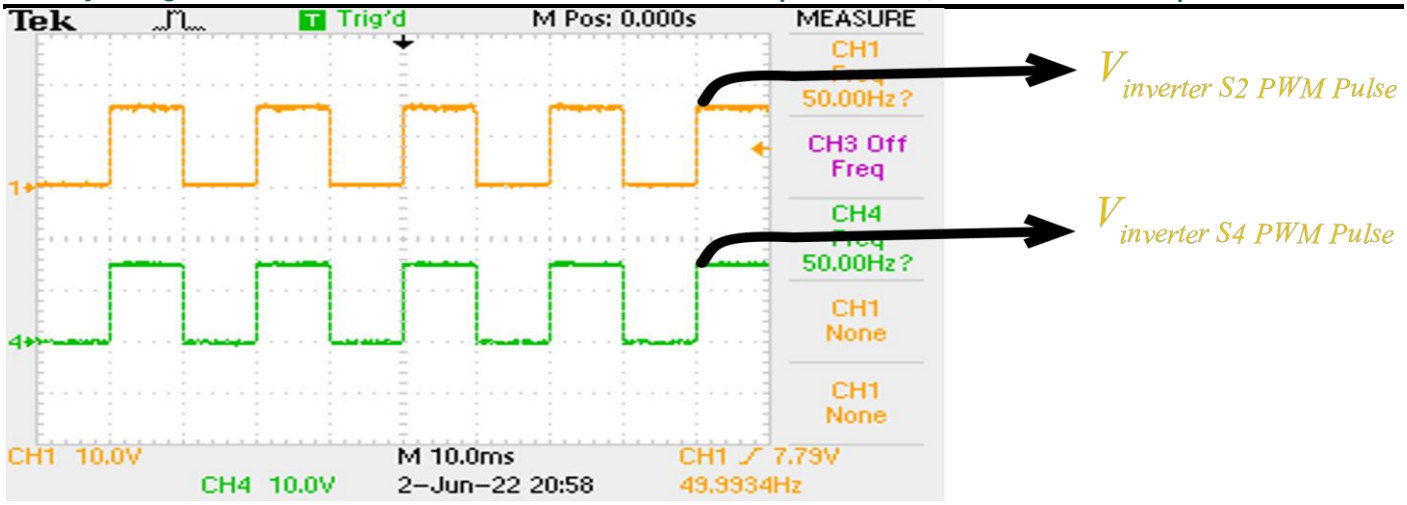

Figure :24 Proposed inverter Gate Pulse for S_2 and S_4

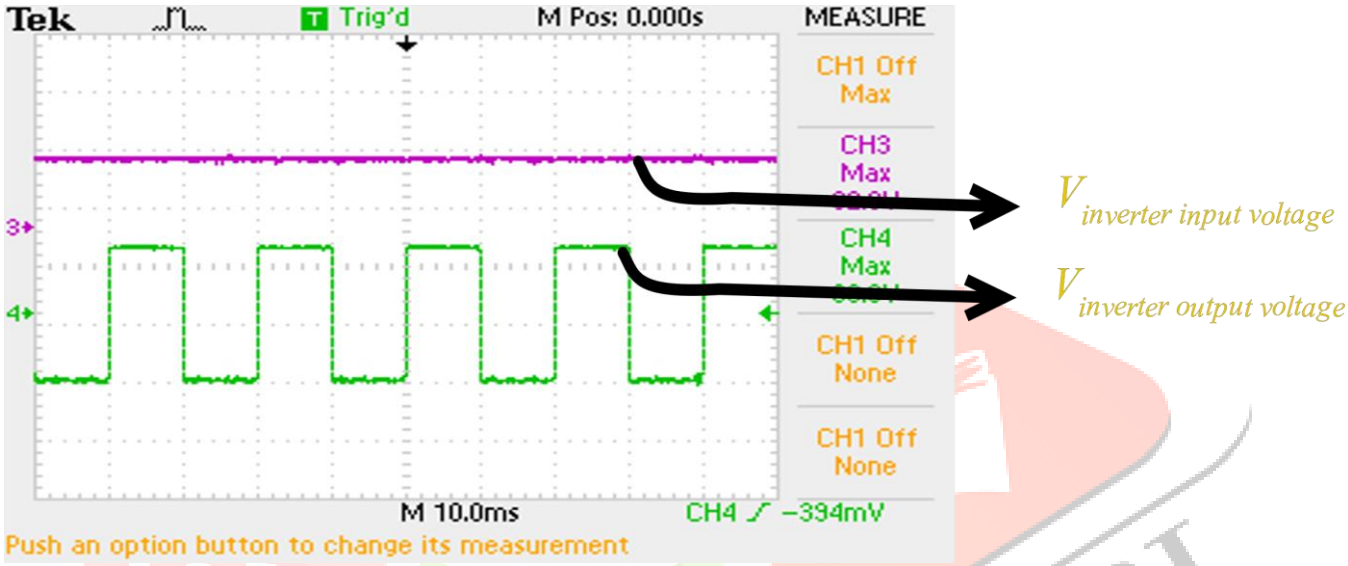

Figure :25 Proposed inverter input voltage and output voltage

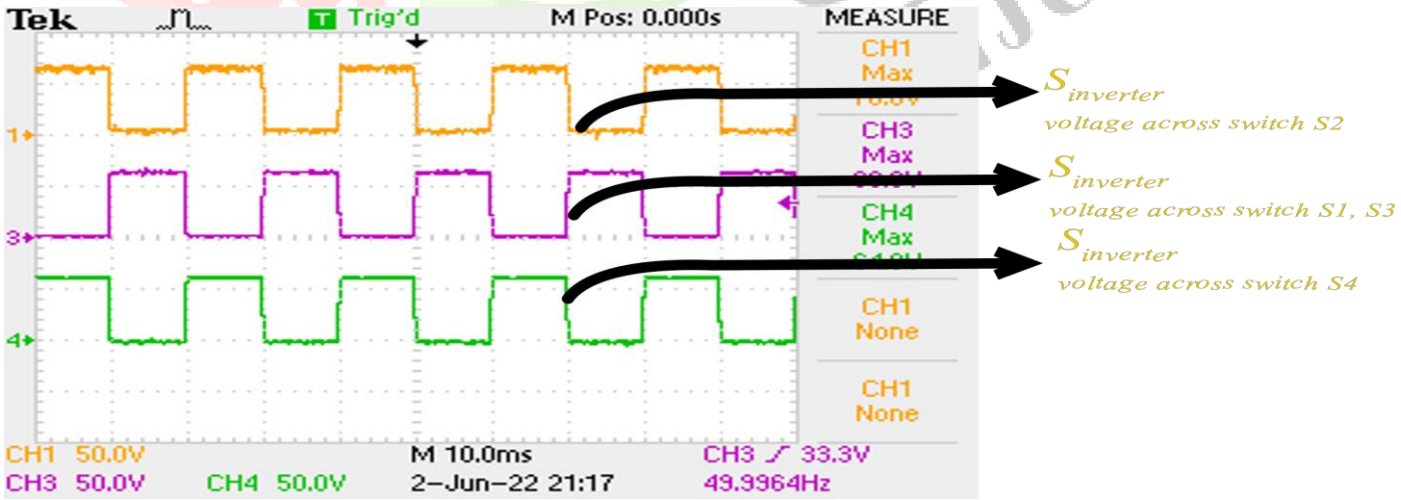

Figure :26 Proposed inverter voltage stress across the switches S_1, S_2, S_3, S_4

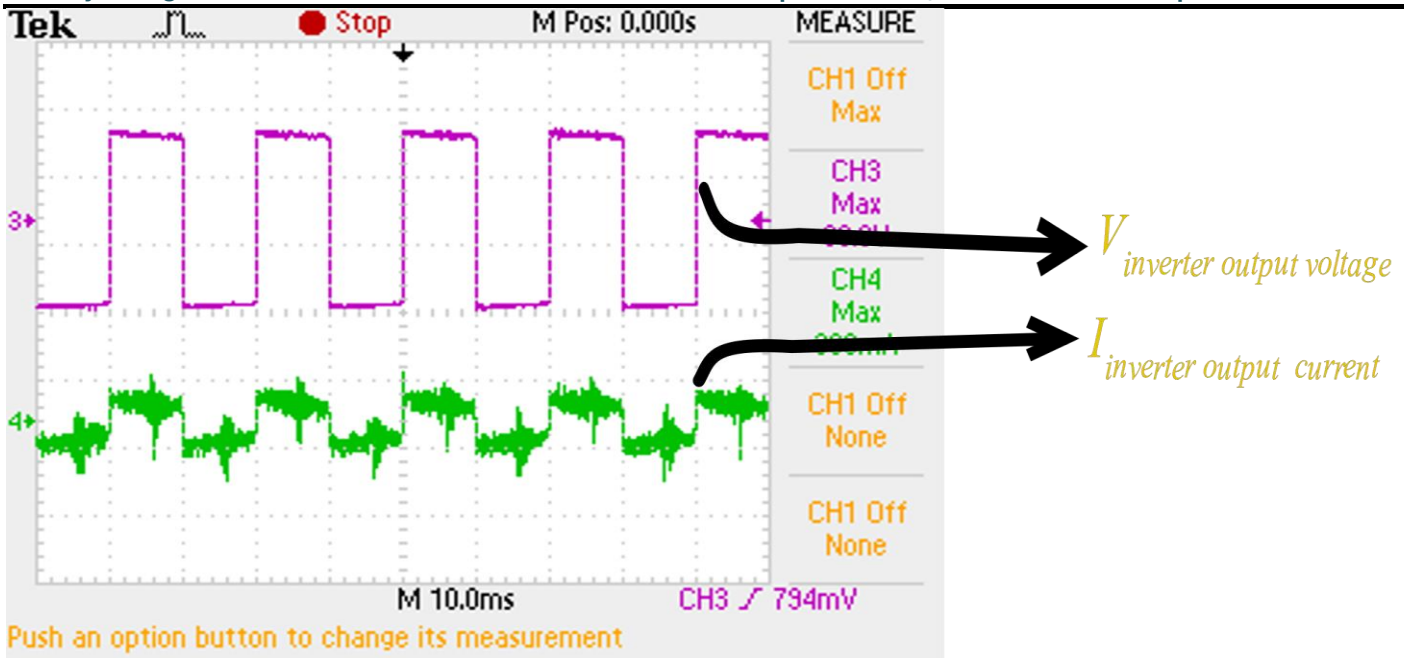

Figure :27 Proposed inverter output voltage and output current

One of the most important parameters of power electronic circuits is their efficiency. Efficiency can be computed by comparing the circuit output power to the power delivered by the supply using the following equation:

$$Eff = \frac{Po}{Pin} = \frac{V0 \times (1-D)^2}{Vin}$$

$$Eff = \frac{173 \times (1-0.5)^2}{45} = 96.11\ \%$$

VIII. VI. CONCLUSION

In this work, fuzzy logic controller-based P&O MPPT and voltage control scheme, PR controller-based voltage and current control scheme has been presented for high stepup DC-DC Quadratic boost converter fed single phase standalone transformer less inverter. The MPPT, modulation index and control strategy and unipolar sinusoidal PWM are simulated by using MATLAB/Simulink and implemented by using the 16-bit DSC dsPIC30f2010. Based on the investigations made from simulation results following important points are concluded. The FLC in Quadratic boost converter side so the results show low oscillation and settling time, low in over shoot, zero steady state error and P&O MPPT have efficiency of 96% at changes in temperature and irradiance. The PR controller in inverter side shows zero steady state error in sinusoidal quantity and low in THDs. In this proposed model a stable DC voltage is supplied to inverter through the Quadratic Boost converter by FLC and a controlled AC output voltage is obtained by adjusting Sinusoidal Pulse Width Modulation through PR controller. The Unipolar SPWM technique improves quality of output voltage, current power. This proposed inverter produces highly efficient AC output successfully.

REFERENCES

[1] Jinia Roy, Yinglai Xia, Rajapandian Ayyanar, 'High Step-up Transformer-less Inverter for AC Module Applications with Active Power Decoupling'.

[2] Muhammad Ammirrul Atiqi Mohd Zainuri, Mohd Amran Mohd Radzi, Azura Che Soh, Nasrudin Abd Rahim, 'Development of adaptive perturb and observe-fuzzy control maximum power point tracking for photovoltaic boost dc–dc converter'.

[3] Lotfi farah, Amir hussain, Abdelfateh Kerrouche, Cosimo Ieracitano, Jamil Ahmad, Mufti Mahmud, "A Highly-Efficient Fuzzy-Based Controller with High Reduction Inputs and Membership Functions for A Grid-Connected Photovoltaic System".

[4] Daniel Zammit, Cyril Spiteri Staines, Maurice Apap, John Licari, "Design of PR Current Control with Selective Harmonic Compensators using MATLAB".

[5] Hanju Cha, Trung-Kien Vu, Jae-Eon Kim, "Design and Control of Proportional-Resonant Controller Based Photovoltaic Power Conditioning System".

[6] S. H. Lee, W. J. Cha, J. M. Kwon, and B. H. Kwon, 'Control strategy of flyback microinverter with hybrid mode for PV ac modules,' vol. 63, no. 2, pp. 995–1002, Feb 2016.

[7] J. Ahmed and Z. Salam, 'A Modified P&O Maximum Power Point Tracking Method with Reduced Steady State Oscillation and Improved Tracking Efficiency', IEEE Transactions on Sustainable Energy, vol. 7, no. 4, pp. 1506-1515, 2016.

[8] H.T. Yau, C.H. Wu 'Comparison of extremum-seeking control techniques for maximum power point tracking in photovoltaic systems', Energies, vol. 4, pp. 2180-2195, 2011.

[9] C. Li, Y. Chen, D. Zhou, J. Liu, J. Zeng, 'A High-Performance Adaptive Incremental Conductance MPPT Algorithm for Photovoltaic Systems', Energies, vol. 9, no. 4, pp. 288, 2016.

[10] H. Rezk, M. Aly, M. Al-Dhaifallah, and M. Shoyama, 'Design and hardware implementation of new adaptive fuzzy logic-based MPPT control method for photovoltaic applications', IEEE Access, vol. 7, pp. 106427–106438, 2019.

[11] V. R. Kota and M. N. Bhukya, 'A novel global MPP tracking scheme based on shading pattern identification using artificial neural networks for photovoltaic power generation during partial shaded condition', IET Renew. Power Gener., vol. 13, no. 10, pp. 1647–1659, Jul. 2019.

[12] W.-M. Lin, C.-M. Hong, and C.-H. Chen, 'Neural-network-based MPPT control of a stand-alone hybrid power generation system', IEEE Trans. Power Electron., vol. 26, Dec. 2011.

[13] J. Roy and R. Ayyanar, 'Sensor-less current sharing over wide operating range for extended-duty-ratio boost converter', IEEE Transactions on Power Electronics, vol. 32, Nov 2017.

[14] A. Kotsopoulos, J. L. Duart, M.A.M Hendrix, "A predictive control scheme for DC voltage and AC current in grid-connected photovoltaic inverters with minimum DC link capacitance", in the 27th annual Conference of the IEEE Industrial Electronics Society, vol.3, pp. 1994- 1999, 2001.

[15] D. G. Holmes and D. A. Martin, "Implementation of a direct digital predictive current controller for single and three phase voltage source inverters", in Proc. 1996 IEEE IAS Annu. Meeting, pp. 906–913.

[16] R. D. Lorenz, T. A. Lipo, and D. W. Novotny, "Motion control with induction motors", in Proc. 1994 IEEE, vol. 82, iss. 8, pp. 1215-1240.

[17] Cha, Hanju, Lee, Sanghoey, "Design and Implementation of Photovoltaic Power Conditioning System Using a Current Based Maximum Power Point Tracking", in Industry Application Society Annual Meeting, pp. 1-5, Oct. 2008.

[18] Guo Xiaoqiang, Zhao Qinglin and Wu Weiyang 'A Single-Phase Grid Connected Inverter System with Zero Steady-State Error', in CES/IEEE 5th International Power Electronics and Motion Control Conference, 2006, vol. 1, pp. 1-5, Aug. 2006.

[19] Zmood, D.N.; Holmes, D.G.; Bode, G., "Frequency domain analysis of three phase linear current controllers", in Industry Applications Conference and Thirty-Fourth IAS Annual Meeting Conference Record of the 1999 IEEE, vol. 2, pp. 818-825.

[20] R. Teodorescu; F. Blaabjerg; M. Liserre and P.C. Loh "Proportional-resonant controllers and filters for grid-connected voltage-source converters", in IEE Proceedings - Electric Power Applications, vol. 153, iss. 5, pp. 750-762, 2006.